



## EVALUATION OF FOUNDATION INPUT MOTIONS BASED ON OBSERVED SEISMIC MOTIONS

O. KURIMOTO

Technical Research Institute, Obayashi Corporation  
4-640, Shimokiyoto, Kiyose-shi, Tokyo 204, JAPAN

M. IGUCHI

Faculty of Science and Engineering, Science University of Tokyo  
2641, Yamazaki, Noda-shi, Chiba 278, JAPAN

### ABSTRACT

Most of experimental studies on soil-structure interaction have been focused on the evaluation of impedance functions that represents the relationship between the dynamic response of rigid foundation and external forces. However, it is important to obtain the foundation input motions as well as the impedance functions to evaluate properly the seismic response of soil-structure system. This paper presents an approximate but practical method to evaluate the foundation input motions based on sparsely observed earthquake ground motions. This method can be applied to practical purpose to evaluate observationally the foundation input motions for structures before construction.

### KEYWORDS

dynamic soil-structure interaction; embedded foundation; foundation input motion; earthquake observation.

### INTRODUCTION

The fundamental quantities in evaluation of soil-structure interaction are the impedance function and foundation input motion. While the analytical studies have preceded the experimental studies, the remarkable improvement of the recent measurement technique has provided the valuable data for clarifying soil-structure interaction effect. Most of experimental studies have been conducted by using the exciter installed on the structure. The results obtained by the force vibration tests include only the effects of "inertial interaction". Therefore, the impedance function can be extracted with a suitable data processing from the vibration test results.

On the other hand, it is impossible to evaluate "kinematic interaction", i.e. the foundation input motion by the forced vibration test. Some studies have tried to estimate the input motions from the earthquake observation results of structures when subjected to seismic waves. However, both "inertial interaction" and "kinematic interaction" are included in such earthquake observation results. The precise estimations of inertial force of structure and impedance function are necessary to separate these interaction effects. Thus, many measurement points must be necessary, and the observation system becomes large as a matter of course.

This paper presents an approximate method to evaluate foundation input motions using free-field displacement records on the premise that impedance functions have been obtained in advance by an experiment or analytical method. The foundation input motions obtained by the proposed method using observed seismic ground motions in absence of any structures are also presented. The proposed method has the advantage of being able to evaluate input motions using earthquake motions recorded with the small observation array.

## APPROXIMATE METHOD FOR FOUNDATION INPUT MOTION

The soil-foundation model considered in this study is shown in Fig. 1. The expression of the input motion for an embedded foundation was presented by Luco (1986) in the form of equation (1).

$$\{U^*\} = [K]^{-1} \int_S [\tau_n^R(\bar{X})]^T \{u^f(\bar{X})\} dS - [K]^{-1} \int_S [A(\bar{X})]^T \{\tau_n^f(\bar{X})\} dS, \quad \bar{X} \in S \quad (1)$$

where  $\{U^*\}$  represents the displacement response of the foundation and consists of three translational and three rotational components for a rigid foundation.

$$\{U^*\} = \{\Delta_x^*, \Delta_y^*, \Delta_z^*, \Phi_x^*, \Phi_y^*, \Phi_z^*\}^T \quad (2-1)$$

$[A]$  is a matrix representing the displacement at  $\bar{X}(x_S, y_S, z_S)$  corresponding to the rigid body motion, and

$$[A(\bar{X})] = \begin{bmatrix} 1 & \cdot & \cdot & \cdot & z_S & -y_S \\ \cdot & 1 & \cdot & -z_S & \cdot & x_S \\ \cdot & \cdot & 1 & y_S & -x_S & \cdot \end{bmatrix} \quad (2-2)$$

$\{u^f\}$  denotes the free-field displacement vector and  $\{\tau_n^f\}$  is the traction vector on the surface  $S$  as defined below.  $S$  means the interface between the embedded foundation and soil,  $\bar{X}(x_S, y_S, z_S)$  expresses the coordinate on  $S$ .

$$\{u^f(\bar{X})\} = \begin{Bmatrix} u_x^f(\bar{X}) \\ u_y^f(\bar{X}) \\ u_z^f(\bar{X}) \end{Bmatrix}, \quad \bar{X} \in S \quad (2-3)$$

$$\{\tau_n^f(\bar{X})\} = \begin{Bmatrix} \tau_{nx}^f(\bar{X}) \\ \tau_{ny}^f(\bar{X}) \\ \tau_{nz}^f(\bar{X}) \end{Bmatrix}, \quad \bar{X} \in S \quad (2-4)$$

$u_x^f, u_y^f, u_z^f$  and  $\tau_{nx}^f, \tau_{ny}^f, \tau_{nz}^f$  means displacements and stress in free-field soil layers. The direction of stress  $\{\tau_n^f\}$  is defined to outside of the region  $S$ .

An alternative form of equation (1) can be expressed by equation (3).

$$\{U^*\} = [K]^{-1} \int_S [A(\bar{X})]^T [Z] \{u^f(\bar{X})\} dS - [K]^{-1} \int_S [A(\bar{X})]^T \{\tau_n^f(\bar{X})\} dS, \quad \bar{X} \in S \quad (3)$$

$[K]$  is the impedance matrix at the bottom center of foundation,  $[Z]$  is the  $3 \times 3$  dynamic stiffness matrix of soil on  $S$ .  $[K]$  is associated with  $[Z]$  as expressed in equation (4).

$$[K] = \int_S [A(\bar{X})]^T [Z] [A(\bar{X})] dS \quad (4)$$

Iguchi (1982) has presented an approximate expression for the input motions as shown in equation (5). The averaging operation for the free-field displacements is taken to the right hand first term of equation (3).

$$\{U^*\} \sim [H]^{-1} \int_S [A(\bar{X})]^T \{u^f(\bar{X})\} dS - [K]^{-1} \int_S [A(\bar{X})]^T \{\tau_n^f(\bar{X})\} dS, \quad \bar{X} \in S \quad (5)$$

where  $[H] = \int_S [A(\bar{X})]^T [A(\bar{X})] dS \quad (6)$

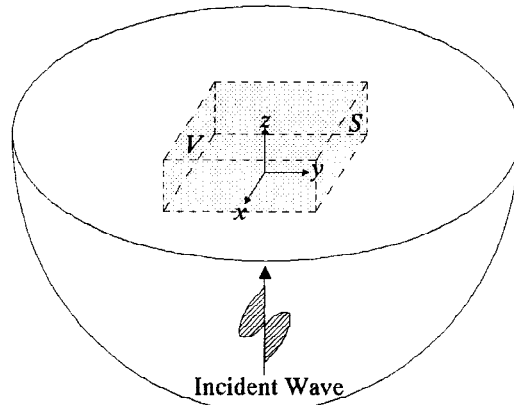


Fig. 1 Description of the problem and Coordinate system

Equations (5) and (6) can estimate the input motions based on the free-field displacements and stresses on the premise that the impedance functions are known in advance. However, it is difficult to measure the stresses accurately in soil layers from the earthquake observation. The objective of this paper is to rewrite equation (3) in term of free-field displacements instead of stresses. The vector  $\{T^f\}$  is introduced by the integral of the right hand second term of equation (5).

$$\{T^f\} = \int_S [A(\bar{X})]^T \{\tau_n^f(\bar{X})\} dS, \bar{X} \in S \quad (7)$$

The components of the vector  $\{T^f\}$  may be expressed as follows.

$$\{T^f\} = \{F_x^f, F_y^f, F_z^f, M_x^f, M_y^f, M_z^f\}^T$$

$F_x^f, F_y^f, F_z^f$  and  $M_x^f, M_y^f, M_z^f$  are the generalized forces and moments by the stresses generated in the free-field soil subjected to the seismic wave. Substitution from equations (2-2) and (2-4) into equation (7) leads to

$$\begin{Bmatrix} F_x^f(\bar{X}) \\ F_y^f(\bar{X}) \\ F_z^f(\bar{X}) \end{Bmatrix} = \int_S \begin{Bmatrix} \tau_{nx}^f(\bar{X}) \\ \tau_{ny}^f(\bar{X}) \\ \tau_{nz}^f(\bar{X}) \end{Bmatrix} dS, \bar{X} \in S \quad (8)$$

$$\begin{Bmatrix} M_x^f(\bar{X}) \\ M_y^f(\bar{X}) \\ M_z^f(\bar{X}) \end{Bmatrix} = \int_S \begin{bmatrix} \cdot & -z_S & y_S \\ z_S & \cdot & -x_S \\ -y_S & x_S & \cdot \end{bmatrix} \begin{Bmatrix} \tau_{nx}^f(\bar{X}) \\ \tau_{ny}^f(\bar{X}) \\ \tau_{nz}^f(\bar{X}) \end{Bmatrix} dS, \bar{X} \in S \quad (9)$$

Making use of the equilibrium law of linear momentum and angular momentum (Mal *et al.*, 1991), equations (8) and (9) may be rewritten in the form of equations (10) and (11)

$$\begin{Bmatrix} F_x^f \\ F_y^f \\ F_z^f \end{Bmatrix} = - \int_V \rho \begin{Bmatrix} \ddot{u}_x^f(X) \\ \ddot{u}_y^f(X) \\ \ddot{u}_z^f(X) \end{Bmatrix} dV, X \in V \quad (10)$$

$$\begin{Bmatrix} M_x^f \\ M_y^f \\ M_z^f \end{Bmatrix} = - \int_V \rho \begin{bmatrix} \cdot & -z & y \\ z & \cdot & -x \\ -y & x & \cdot \end{bmatrix} \begin{Bmatrix} \ddot{u}_x^f(X) \\ \ddot{u}_y^f(X) \\ \ddot{u}_z^f(X) \end{Bmatrix} dV, X \in V \quad (11)$$

where  $\ddot{u}_x^f, \ddot{u}_y^f, \ddot{u}_z^f$  are the accelerations in the free-field,  $V$  means the internal region inside the interface  $S$ ,  $\rho$  means the mass density of soil and  $x, y, z$  show the coordinate in the region  $V$ .

Assuming the steady state with time factor  $e^{i\omega t}$ , equations (10) and (11) can be rewritten in the following form.

$$\begin{Bmatrix} F_x^f \\ F_y^f \\ F_z^f \end{Bmatrix} = \omega^2 \int_V \rho(X) \begin{Bmatrix} u_x^f(X) \\ u_y^f(X) \\ u_z^f(X) \end{Bmatrix} dV, X \in V \quad (12)$$

$$\begin{Bmatrix} M_x^f \\ M_y^f \\ M_z^f \end{Bmatrix} = \omega^2 \int_V \rho(X) \begin{bmatrix} \cdot & -z & y \\ z & \cdot & -x \\ -y & x & \cdot \end{bmatrix} \begin{Bmatrix} u_x^f(X) \\ u_y^f(X) \\ u_z^f(X) \end{Bmatrix} dV, X \in V \quad (13)$$

Substitution from equations (12) and (13) into equation (7) leads to

$$\{T^f\} = \omega^2 \int_V \rho(X) [A(X)]^T \{u^f(X)\} dV, X \in V \quad (14)$$

Therefore, equation (5) can be transformed to equation (15).

$$\{U^*\} = [H]^{-1} \int_S [A(\bar{X})]^T \{u^f(\bar{X})\} dS - \omega^2 [K]^{-1} \int_V \rho(X) [A(X)]^T \{u^f(X)\} dV, \bar{X} \in S, X \in V \quad (15)$$

Equation (15) shows that the input motions can be obtained using the free-field displacements with the a priori impedance functions. Equation (15) also takes more practical form than equation (5).

# EARTHQUAKE OBSERVATION OF SOIL LAYERS

## Characteristics of Observed Earthquake Waves

The earthquake ground motions were observed by seismograms in soil layers as shown in Fig. 2 (Fujimori *et al.*, 1993; Kurimoto *et al.*, 1995). Soil layers consist of loam (shear wave velocities are 90 m/sec. - 125 m/sec.), and rock layers (shear wave velocities are 220 m/sec. - 1200 m/sec.). The backfill sandy soil was controlled so that the shear wave velocity may be 130 m/sec.

The profiles of an observed earthquake used in this study are as follows. The magnitude is 6.5, epicentral depth is 90 Km and epicentral distance is 54 Km. The maximum accelerations for the horizontal-x, horizontal-y and vertical direction at the soil surface are about 75 Gal, 50 Gal and 30 Gal, respectively. Fig. 3 shows Fourier spectra smoothed by Parzen's lag window with the bandwidth of 0.1 Hz in the frequency domain. As seen from Fig. 3, the Fourier spectra at three different points on the soil surface show similar characteristics for the horizontal-x and vertical components, while the different tendency is seen for horizontal-y components. This fact suggests the vertical incidence of the seismic wave.

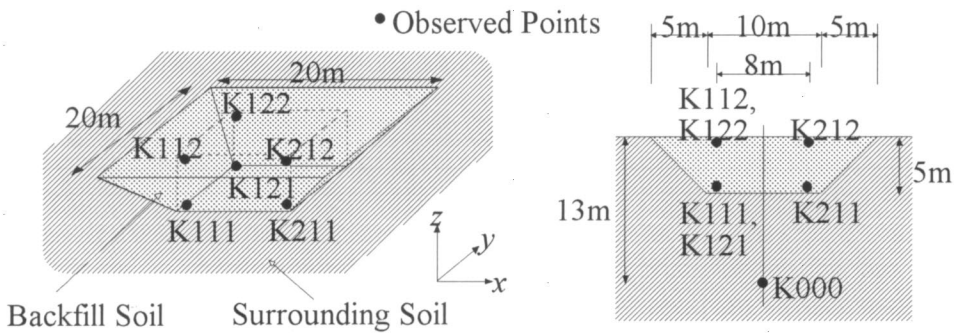


Fig. 2 Location of Seismometers

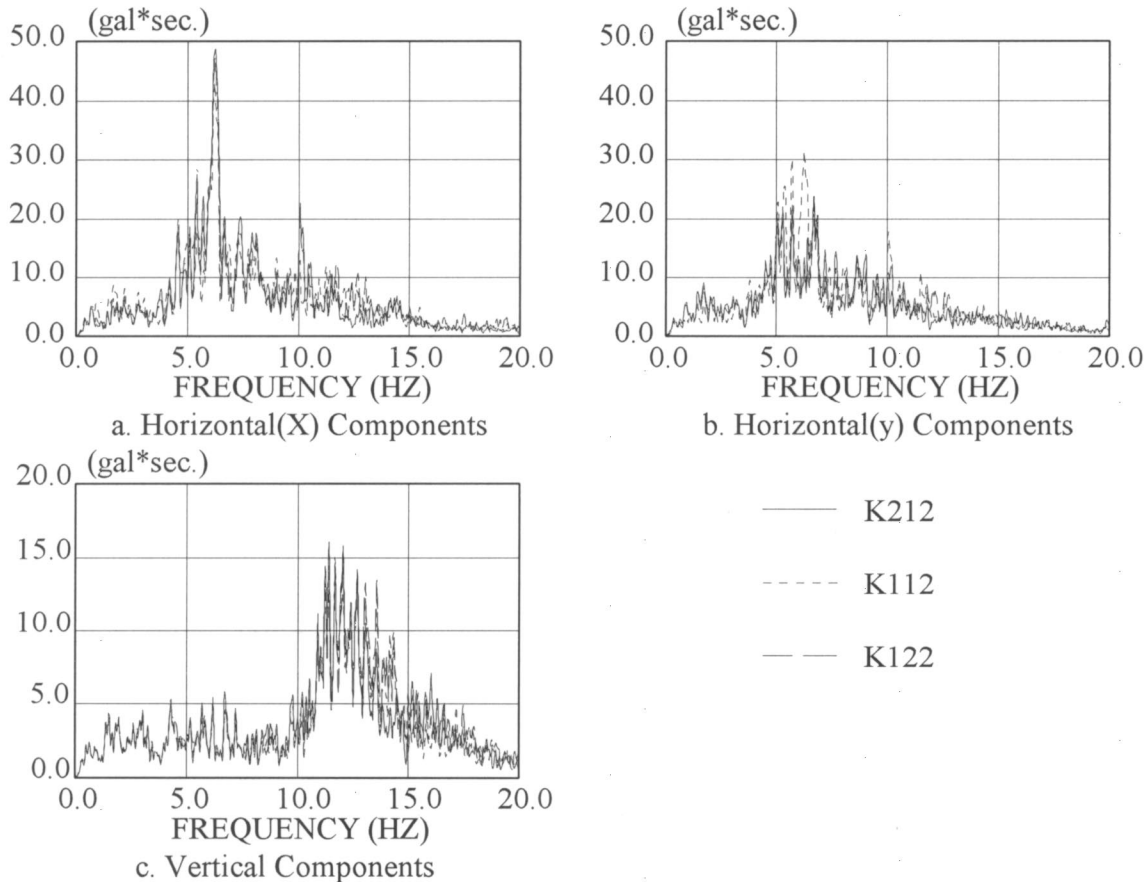


Fig. 3 Fourier Spectra of Observed Earthquake

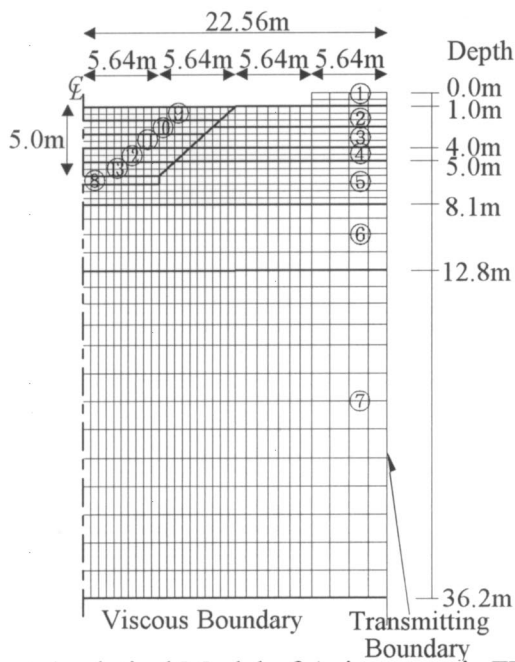


Fig. 4 Analytical Model of Axisymmetric FEM

Table 1 Soil Constants

	Density $\gamma$ (tonf/m <sup>3</sup> )	S Wave Velocity $V_s$ (m/s)	Poisson's Ratio $\nu$	Damping Ratio h (%)	Layer Thickness H (m)
①	1.3	90	0.350	5	1.0
②	1.7	125	0.395	5	1.5
③	1.8	220	0.352	5	1.5
④	1.9	280	0.206	5	1.0
⑤	1.9	280	0.206	5	3.1
⑥	1.9	440	0.328	3	4.7
⑦	2.1	1080	0.412	3	23.4
⑧	1.8	180	0.355	5	0.6
⑨	1.7	110	0.3	5	1.0
⑩	1.7	120	0.3	5	1.0
⑪	1.7	130	0.3	5	1.0
⑫	1.8	140	0.3	5	1.0
⑬	1.8	150	0.3	5	1.0

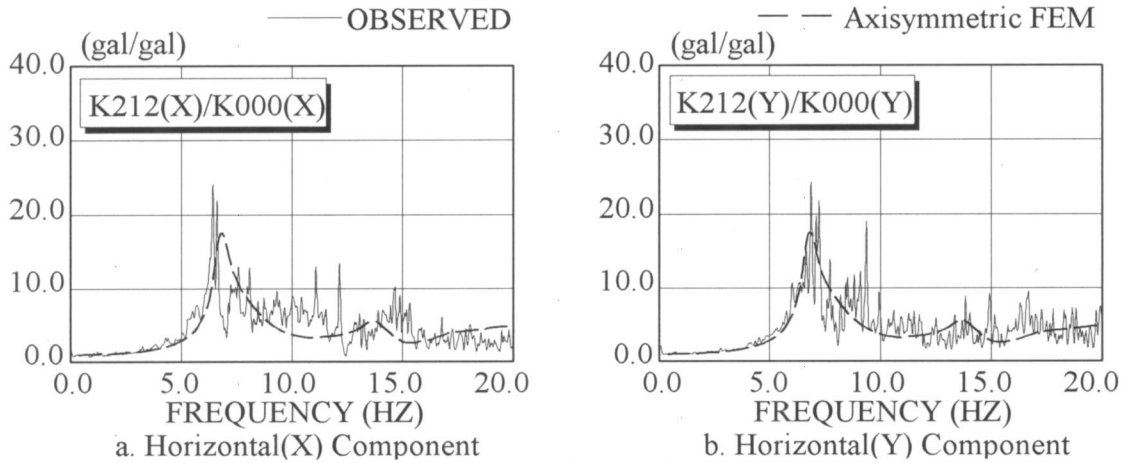


Fig. 5 Comparison of Transfer Functions

### Simulation Analysis of Soil Response

The simulation analysis using axisymmetric finite element method (FEM) was performed to investigate the seismic characteristics of soil. An analytical model of the axisymmetric FEM is shown in Fig. 4 where the square geometry of the actual backfill soil is replaced by the circle with the equivalent area.

The soil constants used in the analysis are shown in Table 1 that were determined based on the boring examinations and elastic wave tests.

Fig. 5 shows the transfer functions comparing the observation with the analysis. The analytical results coincided well with those of observation. The peak frequency of 6.5 Hz may be interpreted as the predominant frequency of the backfill soil and surrounding soil.

### FOUNDATION INPUT MOTIONS USING ACTUAL SEISMIC MOTIONS

A rigid square foundation embedded in the backfill soil is supposed as shown in Fig. 6. It is possible to evaluate approximately the input motions for this foundation using equation (15) provided that the soil displacements and impedance functions are known. Since the forced vibration test was not performed for this observation site, the impedance functions could not be obtained experimentally. Thus, the impedance functions shown in Fig. 7 were used instead, which were calculated by the axisymmetric FEM. The soil properties used for calculating the impedance functions are same as those used in the simulation analysis of the previous section.

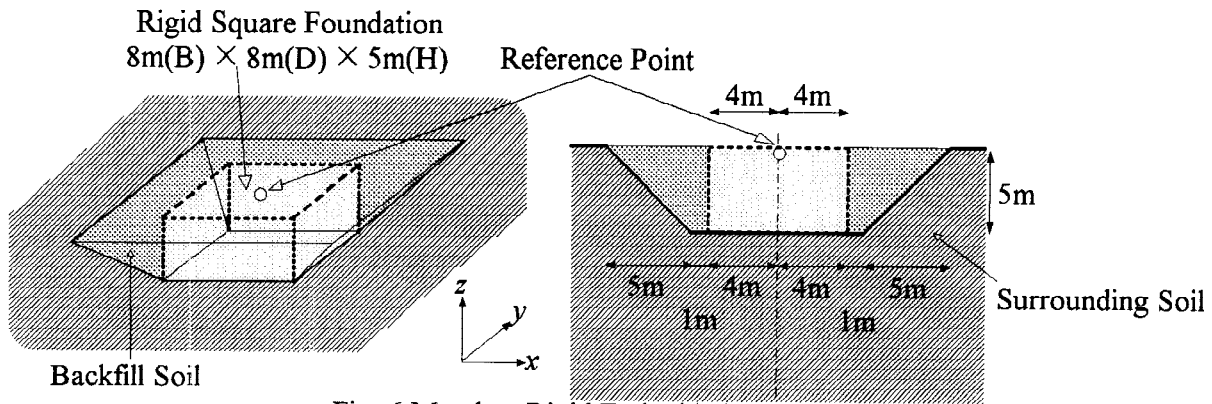


Fig. 6 Massless Rigid Embedded Foundation

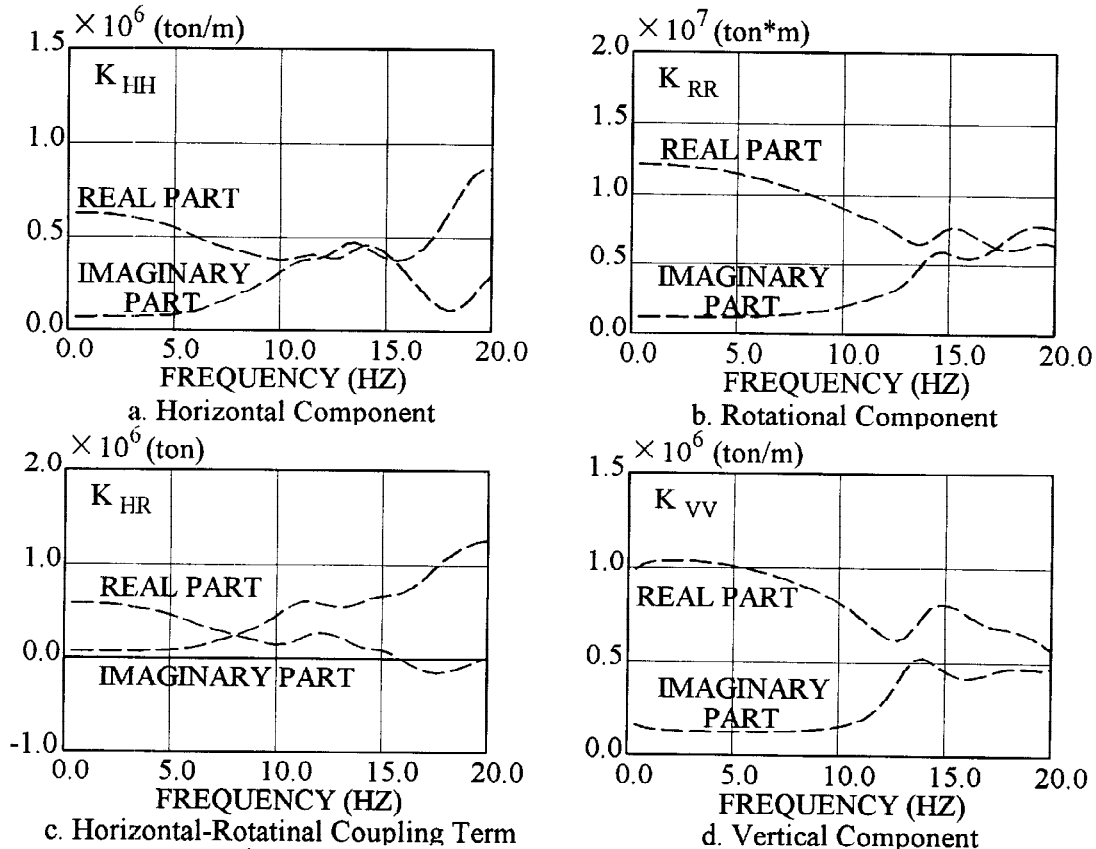


Fig. 7 Impedance Functions by Axisymmetric FEM

Fig. 8 shows the input motions normalized by the response at the reference point that is marked with  $\circ$  in Fig. 6. The input motions indicate that the horizontal components decrease and rotational components increase in the range below 10 Hz. These tendencies are the characteristics of the embedded foundation, and comparable to the existing results (Wong *et al.*, 1978; Luco, 1987). In high frequencies above 15 Hz the accuracy may be degraded lower as the displacement distribution in the domain of the foundation was obliged to assume to be linear because of limited observation points. The characteristics of input motions showed fairly good agreement with analytical results evaluated by the axisymmetric FEM.

The contributions of the first and second term in equation (15) to the input motion are shown in Figs. 9 and 10, respectively. The first term has the large influence in low frequencies below 6 Hz while the contribution of the second term becomes large in high frequencies above 12 Hz.

## CONCLUSIONS

An approximate method to evaluate the foundation input motion and the input motions based on the actual seismic motion have been presented. The characteristics of input motions predicted by the analytical studies

were confirmed by this observational study.

The proposed method has the advantage of being able to evaluate the input motions by using earthquake motions recorded with the small observation array, while another method (for example, Wong *et al.*, 1978) may need a large scale of observation for soil-structure system. The proposed method is also useful in predicting the input motions by using the seismic ground motions of soil layers without any structures, and could be applicable to practical use for seismic response analyses before construction.

### ACKNOWLEDGMENT

The authors wish to express their gratitude to Dr. T. Tsunoda for his support throughout this work.

### REFERENCES

- Fujimori, T., T. Tsunoda, M. Izumi, T. Minami and T. Taira (1993). Seismic responses of embedded structures (Embedment effect tests on soil-structure interaction). *12th SMiRT, K1*, 55-60.
- Iguchi, M. (1982). An approximate analysis of input motions for rigid embedded foundations. *Trans. of A. I. J.*, 315, 61-75.
- Kurimoto, O., T. Tsunoda, H. Kase, K. Akino, T. Minami and M. Iguchi (1995). Input motions for rigid foundations to observed seismic waves. *13th SMiRT, 3, Division K*, 13-18.
- Luco, J. E. (1986). On the relation between radiation and scattering problems for foundations embedded in an elastic half-space. *S.D.E.E.*, 5, 97-101.
- Luco, J. E. and H. L. Wong (1987). Seismic response of foundations embedded in a layered half-space. *E.E.S.D.*, 15, 233-247.
- Mal, A. K. and S. J. Singh (1991). Deformation of elastic solid, *Prentice Hall*, p.99
- Wong, H. L. and J. E. Luco (1978). Dynamic response of rectangular foundation to obliquely incident seismic waves. *E.E.S.D.*, 6, 3-16.

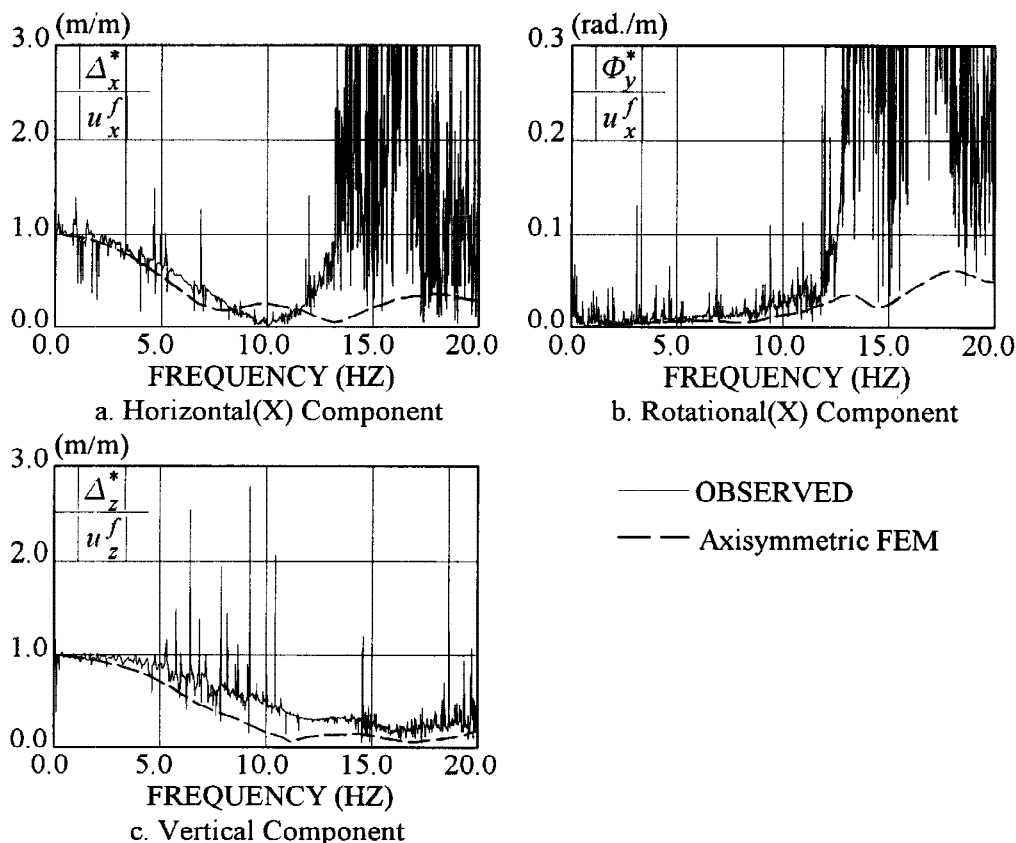
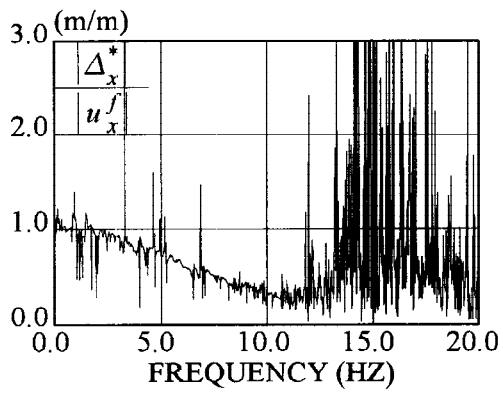
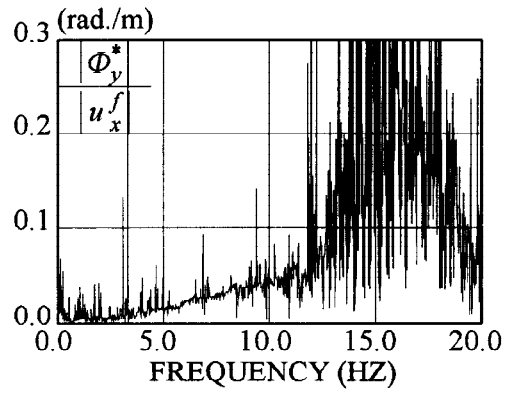


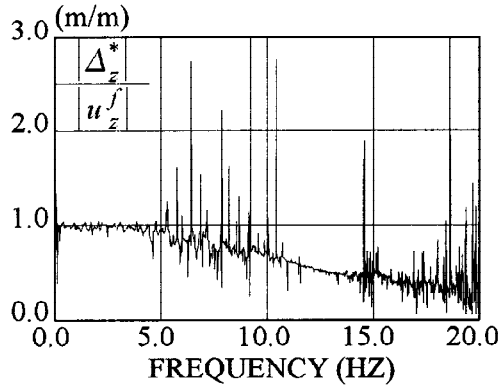
Fig. 8 Foundation Input Motions for Embedded Foundation



a. Horizontal(X) Component



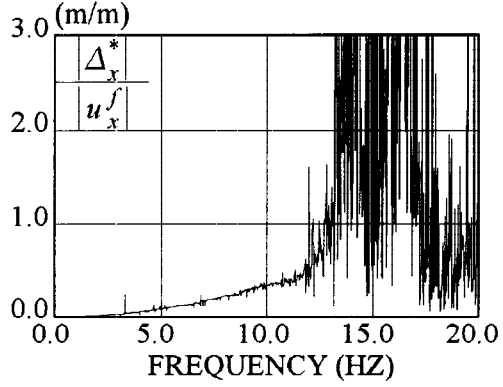
b. Rotational(X) Component



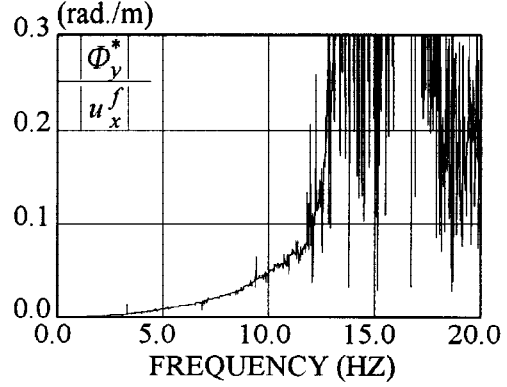
c. Vertical Component

— OBSERVED

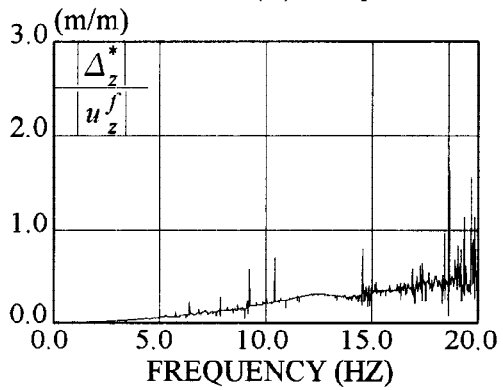
Fig. 9 Foundation Input Motions for Embedded Foundation:  
Contribution of First Term in Equation (15)



a. Horizontal(X) Component



b. Rotational(X) Component



c. Vertical Component

— OBSERVED

Fig. 10 Foundation Input Motions for Embedded Foundation:  
Contribution of Second Term in Equation (15)